 doi:10.20944/preprints201804.0018.v1

Comparative immune-related metabonomics analysis of plasma from mouse after given long-term astragalus membranaceus and panax ginseng

Junqiu Liu[1] , Chen Sha[1], Jun Zhang[1], Jintang Cheng[1], An Liu[1], Guoliang Xu[2*] , Yuesheng Wang[1*]

1 Institute of Chinese Materia Medica, China Academy of Chinese Medical Sciences, No. 16, Nanxiaojie, Dongzhimennei, Beijing 100700, China.

2 Research Center for Differentiation and Development of Basic Theory of TCM, University of Jiangxi TCM, Nanchang, Jiangxi 330006, China.

* Author to whom correspondence should be addressed.

Guoliang Xu, E-mail: xuguoliang6606@126.com; Tel.: +86-791-87118919.

Shengyue Wang, E-mail: yswang@icmm.ac.cn; Tel.: +86-10-64014411.

Abstract

Astragalus membranaceus (AM) and Panax ginseng (PG) are two herbal products with a long history of clinical usage in traditional Chinese medicine (TCM), used in treating a variety of diseases especially in stimulating or inhibiting the immune system. To elucidate the immunity effect of these two traditional Chinese medicine on animal model, four pharmacodynamic indexes (spleen index, thymus index, splenic lymphocyte proliferation and cytotoxic activity of natural killer (NK) cells) were observed on mice. Furthermore, metabolic profiles of plasma were also analyzed by ultra-performance liquid chromatography quadrupole-time-of-flight mass spectrometry (UPLC-Q/TOF-MS, LC-MS) method. All mice were intragastric administrated at three doses (low dose, moderate dose and high dose) once daily for 30 days. Principal components analysis (PCA) and orthogonal projection to latent structure discriminant analysis (OPLS-DA) were performed on LC-MS spectra of plasma, showing that all administration groups developed the disturbance of internal milieu, compared to the blank control (BC) group. Besides, correlation analysis was conducted between pharmacodynamic index and metabolic index. It indicated that uracil, lysoPC(18:3(6Z,9Z,12Z)), sphinganine, LPA(0:0/16:0), UDP-glucuronate, PC(14:0/18:0) were five main endogenous substances, much closely related to four immunological indexes. Glycerophospholipid metabolism was found in both AM and PG groups. Pyrimidine metabolism and sphingolipid metabolism were closely regulated in AM groups. Energy metabolism (starch and sucrose metabolism, Pentose and glucuronate interconversions, together with glycerolipid metabolism) and glycerolipid metabolism were found in PG groups. These findings could contribute to the understanding of mice plasmatic metabolic profiling after long-term administration. Comparative immune-related metabolomic analysis of AM and PG was obtained on the base of pathway analysis of immune-related biomarkers. PG groups trended to have effect on cytotoxic activity of NK cells. AM groups trended to effect thymus index. Our work provides a detailed interpretation of immunological characteristics in different traditional Chinese medicine on metabonomic level.

Keywords: Astragalus membranaceus, Panax ginseng, metabonomics, biomarkers, immune

Preprints (www.preprints.org) | NOT PEER-REVIEWED | Posted: 2 April 2018 doi:10.20944/preprints201804.0018.v1

1. Introduction

Astragalus membranaceus (AM) and Panax ginseng (PG) are two typical Traditional Chinese Medicine (TCM) herbs and they were both listed in 2015 Edition of Chinese Pharmacopoeia. AM has been used to treat a wide range of inflammatory [1], oxidative stress [2], tumor [3], fatigue [4], diabetes and nephropathy [5], immune system [6-11]. Pharmacological studies have shown that PG has the efficacy of anti-cancer [12], blood pressure regulation [13], cognitive recover [14], neuroprotective [15], anti-inflammatory [16], immune system [17, 18]. Both AM and PG could improve fatigue, promote recovery of body and enhance immunity. During thousands of years of clinical practice of TCM, people trend to use these two drugs for tonifying Qi.

It is helpful to build a stable state of internal environment in mice after long-term administration, when compared AM or PG to blank control (BC) group. In this way, it is easy to strengthen the influence of medication on mice and amplify immune-related difference. AM and PG were used to keep in good health state under suitable dosage, acted as a long-term immune regulator in ancient China. Besides, So, we choose this long-term administration model to investigate the influence of AM and PG on mice.

Metabonomic research[19] is an omics approach which uses high-throughput, high-sensitivity and high-precision method to analyze metabolites (biomarkers) in vivo. With the rapid development in application of mass spectrometry, more and more fast, sensitive and reliable qualitative or quantitative metabonomic methods were used to investigate the profiling of small molecules in vivo. Therefore, pharmacological mechanism studies around AM and PG were usually investigated by using metabonomic strategies[20-24]. Some bottlenecks exist however in studying the interpretation of pharmacodynamics by metabonomic method. Besides, these studies were not fully considered as efficacy bias of similar drugs. On the other word, comparative research of AM and PG contribute to discriminate the pharmacological mechanism between them and provide a suggestion in clinical rational drug use.

In the current study, a LC/TOFMS plasma metabonomic method was applied to investigate the biological response in vivo after administration of AM and PG. Furthermore, immune-related pathway was constructed based on the pharmacodynamic index and metabolic index.

2. Experimental design

2.1 Materials and regents

MTT cell proliferation and Cytotoxicity Detection Kit, RPMI 1640 medium (10% newborn bovine serum-10% NBS, penicillin, streptomycin) and RPMI 1640 medium (penicillin, streptomycin) were obtained from Nanjing Keygen Biotech Co., Ltd (Nanjing, China). Concanavalin A (Con A), hank's Balanced Salt Mixture and TRIS were purchased from Beijing Solarbio Science & Technology Co., Ltd (Beijing, China). 10% NP-40 was acquired from Beijing Leagene Biotech Co., Ltd (Beijing, China). YAC-1 cells were obtained from Shanghai Institutes for Biological Sciences of the Chinese Academy of Sciences (Shanghai, China).

Methanol and Acetonitrile of MS grade were purchased from Merck (Merk KGaA, Darmstadt, Germany) and Formic acid used for HPLC-MS analysis from Dikma Technologies Inc., (Beijing, China). Ultrapure water was produced with a Milli-Q water purification system from Millipore (MA, USA). All other reagents used in the present study were analytical grade.

Preprints (www.preprints.org) | NOT PEER-REVIEWED | Posted: 2 April 2018 doi:10.20944/preprints201804.0018.v1

2.2 Animal experiment and sample collection

Eighty-four Institute of Cancer Research (ICR) mice (20 g ± 0.02 g), half male and half female, were randomly divided into BC group , low-dose AM group (LAM, 5 g/kg), moderate-dose AM group (MAM, 25 g/kg), high-dose AM group (HAM, 50 g/kg), low-dose PG group (LPG, 1.5 g/kg), moderate-dose PG group (MPG, 7.5 g/kg) and high-dose PG group (HPG, 15 g/kg). Before drug administration, the mice were acclimatized for 7 days in a rearing environment with 12 h light-dark cycle (light on from 6:00 to 18:00 h) at ambient temperature (22-24°C) with 60% relative humidity. Mice were fasted for 12 h with free access to water. They were fed continuously for 30 days by intragastric administration of AM or PG. After administration, serial blood samples (about 1.00 mL) were collected by eyeballs extraction into heparin-containing tubes and centrifuged at 3000 rpm for 15 min. Plasma was separated and stored at -20 °C until analysis. Furthermore, another two studies were performed, which were splenic lymphocyte proliferation assay and cytotoxic activity of natural killer (NK) cells assay. All experimental procedures were approved by the Institutional Animal Care Committee of Chinese Academy of Medical Sciences.

2.2.1 Splenic lymphocyte proliferation assay

Mouse spleen was removed, grinded and passed through a stainless mesh (200Φ) by aseptic operation. The final concentration of spleen suspension cells (SSCs) was adjusted to 3×10^6/mL by RPMI1640 medium containing 10% NBS (ratios of living cells was 96%-98% by trypan blue exclusion).

Spleen suspension cells (1 mL per well) proliferation were stimulated by Con A (final concentration 3.0 μg/mL) in 24 well cell culture cluster and then cultured at 37 °C in 5% CO_2 cultivating box for 68 h. After 68 h incubation and then centrifuged at 1000 rpm/min for 10min. The supernatant was discarded and the same volume of RMPI 1640 medium without 10% NBS was added into each well. Subsequently, MTT solution (5mg/mL) was added into the wells with a volume of 100 μL per well, and intermixed into uniformity softly, put it into 5% CO2 cultivating box again. After another 4 h incubation and then centrifuged at 4200 rpm for 10 min. 500 μL supernatant was discarded and 800 μL dimethyl surtoxide (DMSO) was added into each well. The absorbance was measured at 570 nm by Enzyme Mark Instrument, and the average optical density (OD) value was calculated. The stimulation index (SI) was calculated according to the following formula: $SI = OD_{\text{Con A stimulated lymphocyte proliferation}} - OD_{\text{spontaneous lymphocyte proliferation without Con A}}$. SI was used to assess the difference of proliferation ability between treatment groups and BC group.

2.2.2 Cytotoxic activity of natural killer cells assay

Yac-1 cells were used as target cells and washed by hank's solution three times in pre-experiment. Finally, the concentration of target cells was adjusted to 4×10^5/mL by RPMI1640 medium containing 10% NBS (ratios of living cells was 98% by trypan blue exclusion).

SCCs were collected by the same method in splenic lymphocyte proliferation assay. After speed centrifugation at 1000 rpm/min for 10 min, 500 μL sterile water was added to splitting erythrocyte for 20 seconds and then 8.0 mL hank's solution was added. Finally, the concentration of cells was adjusted to 2×10^7/mL by RPMI1640 medium containing 10% NBS (ratios of living cells was 97% by trypan blue exclusion).

SCCs without erythrocyte were regarded as effector cells. Equivalent amount (100 μL) of RPMI1640 medium, 1% NP40 solution and effector cells were added into the wells with 100 μL

Preprints (www.preprints.org) | NOT PEER-REVIEWED | Posted: 2 April 2018 doi:10.20944/preprints201804.0018.v1

target cells in 96 well cell culture cluster, respectively. At 50:1 effector-target ratio, the lytic activity of NK cell was investigated. Three independent experiments ran in duplicate. After 4 hours incubation in 5% CO_2 cultivating box, centrifuged at 1500 rpm/min for 10 min and 100 μL lactic dehydrogenase solution (LDH) was added to the supernatant. LDH contained lithium lactate (5×10^{-2} mol/L), iodonitrotetrazolium (INT, 6.6×10^{-4} mol/L), phenazine methosulfate (PMS, 2.8×10^{-4} mol/L) and nicotinamide adenine dinucleotide (NAD, 1.3×10^{-3} mol/L). The reaction was stopped by 1mol/L HCl. The absorbance was measured at 490 nm by Enzyme Mark Instrument, and the average optical density (OD) value was calculated.

NK activity=(experimental-spontaneous release)/(maximum- spontaneous release)*100%

2.2.3 Viscera index analysis

Spleen and thymus of mice were stripped under sterile environment, weighted and calculated after the last administration. Spleen index was calculated by spleen weight (mg) divided / weight (g). Thymus index was calculated by thymus weight (mg) / body weight (g).

2.2.4 Sample preparation for metabolite profiling

Plasma samples were thawed at room temperature and 100 μL of plasma sample was transferred into an eppendorf tube, and then 300 μL of ice-cold acetonitrile was added to precipitate the plasma proteins. Samples were then vortexed for 1 min and stored in refrigerated (4°C) condition for 3 hours. After that, centrifuged at 16,000 rpm for 15 min (4°C) and the supernatant was transferred and evaporated to dryness under a vacuum centrifugal concentrator. The residue was reconstituted in 200 μL of 15% acetonitrile–water, and a 1 μL aliquot was injected for analysis.

2.3 Validation of the metabonomic method

Reproducibility and precision of method were investigated. Relative standard deviation (RSD) of detected retention time, mass-to-charge ratio (m/z), peak height and peak intensity were investigated. Typical pooled samples were used as analysis object for quality control (QC). 72 pooled plasma samples were mixed together of equal volumes (10 μL) and prepared as Sample Preparation method.

2.4 LC-MS and LC-MS/MS platforms for metabolite profiling

UPLC analysis was conducted on a 1290 UPLC system (Agilent Technologies, Santa Clara, CA, USA). Injection volume was 1.0 μL and the flow rate of the mobile phase was 0.40 mL/min. Separation of analytes was performed on a reversed phase Agilent Zorbax XDB-C_{18} column (2.1 mm × 50 mm, particle size 3.5 μm) with the column oven set to 35 ◦C. The elution gradient was eluted from the column under a gradient of 0.1% v/v formic acid in water (A) and acetonitrile (B) and optimized separation was obtained according to a linear gradient (0-1.5 min, 5% B; 1.5-3 min, 5-50% B; 3-16 min, 50-95% B; 16-21 min, 95% B, returned to 5% B for 5 min). Acetonitrile as a blank solution was run every four samples.

Mass spectrometry was performed by using a time-of-flight mass spectrometer (Q-TOF-MS/MS, 6538 UHD Accurate Mass Q-TOF; Agilent Technologies) equipped with an electrospray ionization source, operated in positive-ion and negative-ion modes. MS conditions: Capillary voltage, 4000 V (+) and 3500V (-); Gas temperature, 350 °C; Flow rate of drying gas (N_2), 10 L/min; Nebulizer

Preprints (www.preprints.org) | NOT PEER-REVIEWED | Posted: 2 April 2018 doi:10.20944/preprints201804.0018.v1

pressure, 35 psi; Skimmer voltage, 50 V; Octopole radiofrequency, 150 V; Fragmentor voltage, 150 V; Mass range, 30-1100 Da. The data were collected in profile mode using the internal reference mass for accurate, automated mass calibration correction during LC/MS runs. Purine (*m/z* 121.050873) and HP-0921 (*m/z* 922.009798) were used as internal reference masses in positive ion mode, and in negative ion mode were TFA anion (*m/z* 112.985587) and HP-0921 (*m/z* 1033.988109). The reference nebulizer was set at 1 psi. The MS/MS spectra of potential biomarkers were obtained by UPLC-MS/MS method in target mass mode. Ultra-performance liquid chromatography method was the same as this in LC-MS method. Collision energy were set at 10, 20 and 40 eV, respectively.

2.5 Data Processing

The collected raw data were extracted and analyzed by the function of Molecular Feature Extractor (MFE) within MassHunter Qualitative Analysis (Agilent Technologies). The retention time, *m/z* value, and the volume for each compound were investigated. The data were converted into the .cef format by Agilent MassHunter Profinder (AMP, Agilent Technologies) for targeted recursive feature finding, for peak detection and alignment. And then, .cef data were imported into Mass Profiler Professional (MPP, Agilent Technologies) for differential analysis. To compare the metabolite profiles among BC, AM and PG groups, the Student's t-test and analysis of variance were conducted. Compounds with the value of $p < 0.05$ and fold change ≥2.0 were selected as preliminary potential biomarkers. Then, the biomarker formulations were generated and queried using the Agilent METLIN Compound Database (assistant software package in MPP).

PCA and OPLS-DA models were performed by SIMCA-P 14.1 (Umetrics, Umea, Sweden). Variable importance in the projection (VIP) values was taken as key point for peak selection. Student's t test was used to measure the significance of each metabolite. Metabolites of VIP value larger than 1.0 (VIP>1.0, $p<0.05$) was considered as characteristic metabolites. The typical fragmentation patterns of selected biomarkers were analyzed based on the MS/MS data information.

Besides, the metabolic pathway analysis of proposed biomarkers was analyzed by MetaboAnalyst3.0 with KEGG (http://www.genome.jp/kegg/) and the Human Metabolome Database (http://www.hmdb.ca/). Based on the obtained pathway information, a cross-over analysis of identified biomarkers was analyzed comprehensively, using related references.

Correlation analysis was conducted by using SPSS 24.0 for Windows (IBM, Armonk, NY, USA). Pearson's correlation coefficient was used to investigate correlations between the four pharmacodynamics indexes and identified biomarkers, to find out immune-related biomarkers.

3. Results and discussion

3.1 Method validation

A rigorous data and complete analysis of experiment are in close with the application of optimized method. So, it is necessary to do an evaluation of analysis method in pre-experiment to assure repeatability and precision of plasma sample analysis. To investigate the reproducibility of untargeted analyses of plasma, we performed 40 repeat analyses on a 1.0 μL injected volume of a single QC sample and analyzed the acquired data. Ten ions in positive and tent ions in negative mode were chosen as targeted ions. The RSD value was calculated as a measurement of method

Preprints (www.preprints.org) | NOT PEER-REVIEWED | Posted: 2 April 2018 doi:10.20944/preprints201804.0018.v1

repeatability. Besides, intra- and inter-day biological variations were used to determine the precision of the proposed method. Twelve replicates of the QC samples were analyzed within one day and inter-day variability test was conducted in consecutive 3 days. Variations were represented by RSD. These were shown in Table 1.

Preprints (www.preprints.org) | NOT PEER-REVIEWED | Posted: 2 April 2018 doi:10.20944/preprints201804.0018.v1

Table 1 Repeatability and precision of twenty targeted ions (ten positive ions and ten negative ions)

Target ions		**Repeatability / % (RSD, n=40)**				**Precision Intra-day / % (RSD, n=12)**				**Precision Inter-day / % (RSD, n=12)**			
Rt	m/z	Rt	*m/z*	Height	Intensity	Rt	*m/z*	Height	Intensity	Rt	*m/z*	Height	Intensity
0.58	203.0529	0.14	1.48×10^{-5}	3.98	2.32	0.16	2.22×10^{-5}	2.23	1.12	0.25	1.41×10^{-5}	2.44	3.12
1.47	120.0809	0.22	4.45×10^{-5}	2.97	2.28	0.18	3.53×10^{-5}	1.34	1.32	0.05	2.76×10^{-5}	4.53	2.12
2.73	188.0709	0.27	5.75×10^{-5}	4.82	2.64	0.22	2.11×10^{-5}	3.56	3.32	0.05	3.24×10^{-5}	2.53	4.37
5.71	520.3401	0.05	4.02×10^{-5}	3.50	7.72	0.04	3.25×10^{-5}	2.31	3.43	0.03	2.81×10^{-5}	1.89	2.31
5.96	568.3403	0.04	5.78×10^{-5}	2.47	1.50	0.06	3.16×10^{-5}	3.56	2.65	0.03	1.09×10^{-5}	3.68	3.18
5.98	544.3405	0.04	2.97×10^{-5}	1.89	1.47	0.01	3.25×10^{-5}	2.43	5.31	0.04	2.35×10^{-5}	3.88	2.56
6.23	496.3404	0.04	4.59×10^{-5}	3.15	3.80	0.02	2.18×10^{-5}	1.78	1.12	0.07	1.75×10^{-5}	2.31	2.21
6.58	546.3556	0.05	5.09×10^{-5}	1.96	5.33	0.02	3.11×10^{-5}	2.32	4.45	0.15	2.12×10^{-5}	2.81	2.31
7.03	522.3558	0.07	9.87×10^{-5}	1.62	4.03	0.03	2.23×10^{-5}	2.87	2.78	0.20	3.97×10^{-5}	3.40	2.81
8.21	524.3712	0.08	4.17×10^{-5}	3.21	4.93	0.04	2.45×10^{-5}	2.35	1.98	0.14	1.91×10^{-5}	2.03	2.65
3.53	321.0440	0.19	8.97×10^{-5}	2.23	6.57	0.11	6.12×10^{-5}	1.32	3.43	0.13	2.28×10^{-5}	1.67	1.91
5.83	476.2789	0.14	4.78×10^{-5}	3.67	4.08	0.13	3.46×10^{-5}	2.56	2.15	0.05	3.32×10^{-5}	4.70	3.72
6.22	540.3314	0.11	3.12×10^{-5}	1.23	4.79	0.15	4.21×10^{-5}	2.89	2.27	0.06	1.36×10^{-5}	2.38	2.09
6.52	530.3026	0.13	6.35×10^{-5}	1.41	2.28	0.17	3.88×10^{-5}	2.34	3.39	0.15	2.86×10^{-5}	1.88	1.61
7.41	295.2284	0.06	2.19×10^{-5}	2.21	2.83	0.08	3.32×10^{-5}	3.54	3.51	0.10	1.19×10^{-5}	2.12	2.31
8.20	568.3628	0.11	8.07×10^{-5}	3.28	3.27	0.09	4.51×10^{-5}	1.98	2.29	0.11	5.20×10^{-5}	2.83	2.28
8.59	558.3337	0.13	4.73×10^{-5}	2.78	3.26	0.08	2.32×10^{-5}	1.21	1.21	0.15	3.51×10^{-5}	4.07	2.41
12.31	327.2335	0.02	6.12×10^{-5}	2.45	2.07	0.05	5.78×10^{-5}	1.32	4.10	0.02	2.19×10^{-5}	4.40	1.63
14.27	255.2331	0.01	5.80×10^{-5}	3.45	2.12	0.02	2.12×10^{-5}	2.48	2.38	0.04	3.28×10^{-5}	3.88	2.82
14.69	134.8945	0.01	3.15×10^{-5}	2.89	8.07	0.02	2.76×10^{-5}	1.43	4.41	0.02	1.24×10^{-5}	3.55	2.21

Preprints (www.preprints.org) | NOT PEER-REVIEWED | Posted: 2 April 2018 doi:10.20944/preprints201804.0018.v1

3.2 Pharmacodynamics evaluation of immune index in mice

3.2.1 Effect of AM and PG on mice weight and viscera index

There was no significant difference in the body weights of mice between treatment groups and BC group in Figure 1A. Besides, no significant difference was also found in thymus index in Figure 1B. The index numbers of spleen of MPG, HPG, LAM and MAM groups were significantly higher than BC group (p<0.05) in Figure 1C. It showed that long-term administration of AM or PG contributed to strengthen the spleen index of mice, compared to the BC group.

3.2.2 Effect of AM and PG on the proliferation of splenic lymphocytes

The SI in treatment groups with AM and PG all showed a significant increase as compared with that in BC group in Figure 1D. It indicated that AM and PG improved adaptive immunity in mediating proliferation of splenic lymphocytes.

3.2.3 Effect of AM and PG on the cytotoxic activity of NK cells

Compared to BC group, the spontaneous lymphocyte-mediated cytotoxicity of spleen against YAC-1 target cells were increased by 71.74% in LPG (p<0.01) and increased by 48.67% in LAM groups in Figure 1E. It indicated that AM and PG improved innate immunity in mediating cytotoxic activity of NK cells.

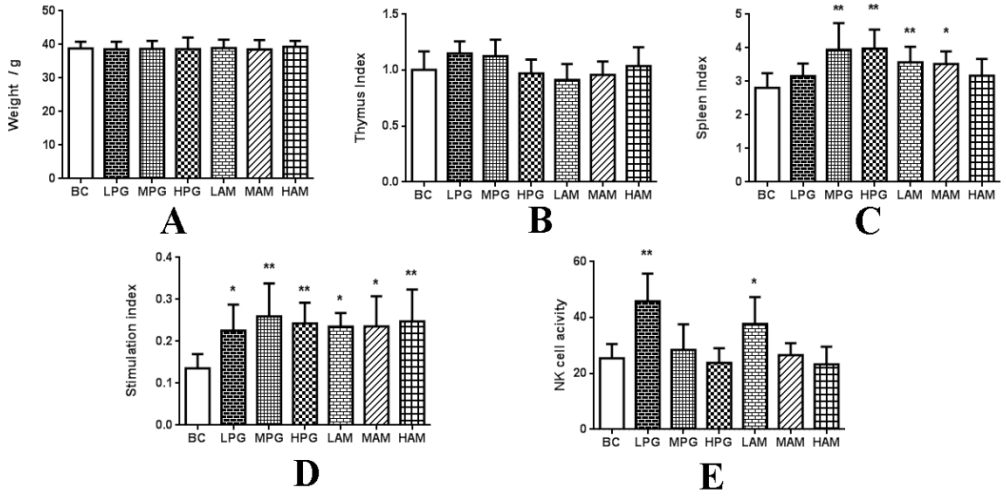

Figure 1: Pharmacodynamics evaluation of immune index in mice. **A.** Weight of BC and administration groups. **B.** Thymus index of BC and administration groups. **C.** Spleen index of BC and administration groups. **D.** Proliferation ability of BC and administration groups. **E.** NK cell activity of BC and administration groups. All these results were expressed as mean ± SD. ** represents p <0.01, * represents p <0.05, compared with the BC group (n = 12).

The behavior of immune system function is a comprehensive reflection of immune organs and cells in *vivo*. Once physiological equilibrium is broken by internal or external factors, numerous functional and phenotypic changes in monocytes, macrophages, T and B-lymphocyte cells may happened.

In general, spleen and thymus are two important immune organs in *vivo*. Spleen is the biggest immune organ with a plenty of lymphocytes and macrophages, which accounting for 25 percent of

Preprints (www.preprints.org) | NOT PEER-REVIEWED | Posted: 2 April 2018 doi:10.20944/preprints201804.0018.v1

weight in total lymphatic tissues. As a central immune organ, spleen is responsible for both humoral and cellular immunity. Thymus is a place that lymphocytes differentiate, grow and mature. The results indicated that AM or PG may improve immune activities by increasing spleen index rather than thymus index. Spleen is used a reservoir of blood and clears aged erythrocytes to improve the blood circulation. In this way, blood may play an important role in regulating immune system.

During the early phases of infections, innate immune response is triggered prior to adaptive immune response. NK cells are quickly gained from blood circulation and fight with target cells such as tumor cells[25], virus-infected cells [26] and parasite [27]. In this way, down-stream adaptive immune response is strengthened [28]. From the data of NK cell activity assay, the NK cell activity increased in both AM and PG groups with significant difference. In splenocyte proliferation assay, splenocyte proliferation also increased. Long-term administration of AM and PG had a demonstrable positive effect on innate and adaptive immune. Our work was in compliance with previous studies, which AM and PG could improve immune system in normal and disease mode[18, 29].

3.3 Untargeted metabolomic profiling of mice plasma

3.3.1 Screening and discovery the biomarkers of AM and PG

AM and PG are widely used in improving immunity in China. To explore the difference of immune response between them in metabonomic level, we conducted an integrated metabonomic investigation of mice plasma by LC-MS/MS method.

A global analysis of metabonomic is untargeted discovery of AM- and PG-induced changes in the diversity of small molecules or endogenous substance in plasma samples. All detected compounds (known or unknown) in plasma samples were taken into investigation by LC-MS method. The typical total ion current (TIC) chromatograms of quality control (QC) samples containing AM and PG groups were shown in Figure 2. The data (2176 variables) were used for multivariate statistical analysis.

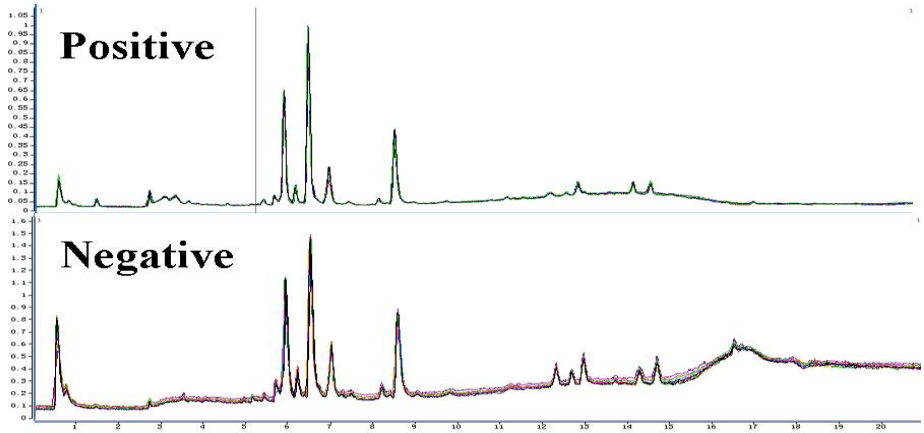

Figure 2 Typical UPLC/Q-TOF MS total ion current chromatogram of quality control samples in ESI positive and negative ion mode.

Preprints (www.preprints.org) | NOT PEER-REVIEWED | Posted: 2 April 2018 doi:10.20944/preprints201804.0018.v1

The normalized metabonomic data obtained from UPLC-Q-TOF MS/MS profile data (acquired in positive-ion and negative-ion modes) was processed by MPP software and imported into SIMCA-P software (Version 14.1, Umetrics AB, Sweden) for multivariate data analysis. Unsupervised PCA and supervised OPLS-DA models were made based on LC-MS-acquired data to clarify the metabolic changes and identify the metabolites of BC and treated groups.

In positive ion mode, there were 2160 variables in AM groups and 1714 variables in PG groups. In negative ion mode, there were 768 variables in AM groups and 717 variables in PG groups. All those variables were analyzed using PCA model with auto-scaling. AM (LAM, MAM, HAM) groups and BC group were separated into distinct clusters in PCA model in Figure 3A (positive) and 3C (negative), respectively. There were some partial overlaps among AM groups in negative ion mode. PG (LPG, MPG, HPG) groups and BC group were also separated into distinct clusters in PCA model in Figure 3E (positive) and 3G (negative), respectively. But there were overlaps to a large extent between MPG and HPG groups. It presented good similarity of various rats in the same group and good separation between BC and treated groups according to the information of PCA scores plot.

Metabolic profiling of plasma in treated mice was much different from those of the BC mice. To reduce the individual differences and make a further investigation into those metabolites, which were much close to the separation between the treated and BC groups. OPLS-DA models were built and applied to identify potential biomarkers on the base of the principal components PC1, PC2 and PC3. Score plot represented clear separation of treated and BC groups in Figure 3B, 3D, 3F and 3H. The validation plot Figure 3I, 3J, 3K and 3L with 200-iteration permutation test indicated that OPLS-DA models were valid and the permutated values were significantly lower than un-permutated original values. The potential biomarkers between treated and BC groups were screened by VIP values (>1) of OPLS-DA model, together with value of $p < 0.05$ and fold change ≥2.0. Endogenous metabolites were found in AM groups and in PG groups, compared to BC group. Furthermore, the identification of metabolite was confirmed by fragmentation of previously detected ions by target mass spectrometry. The detail information was showed in Table 2.

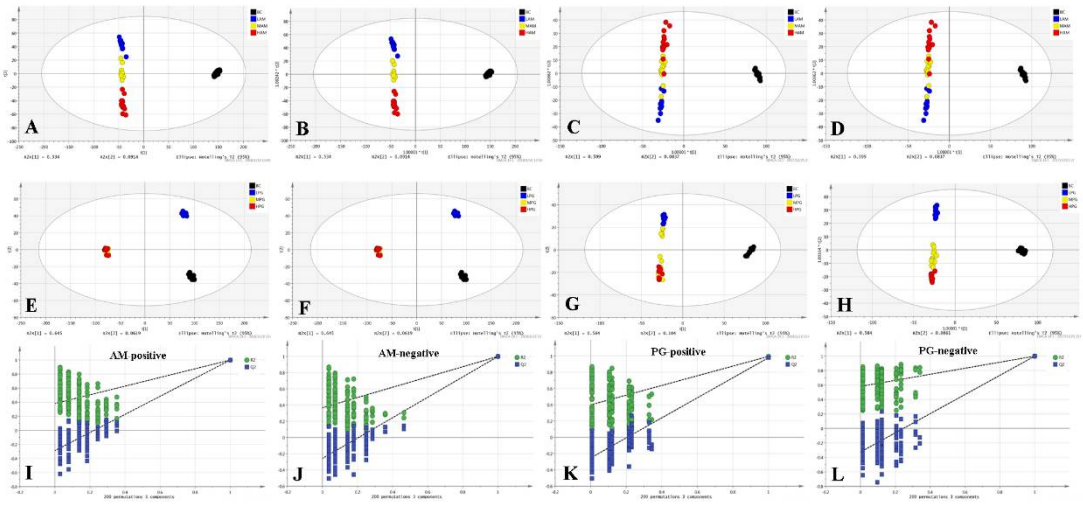

 doi:10.20944/preprints201804.0018.v1

Figure 3 Plasmatic metabolic-profiling analysis of mice in the AM and PG groups during 30 days. A, C, E and G were principal component analysis (PCA) score plots; B, D, F and H were partial least-squares discriminant analysis (OPLS-DA) score plots; I, J, K and L were repeated permutation tests.

Preprints (www.preprints.org) | NOT PEER-REVIEWED | Posted: 2 April 2018 doi:10.20944/preprints201804.0018.v1

Table 2 Biomarkers identified in AM and PG groups by UPLC-Q/TOF-MS

Group	Identify	Rt (min)	m/z (mode)	Formula	VIP	Log FC	Low	Moderate	High
AM	Uracil	0.76	113.0342 (+)	$C_4H_4N_2O_2$	1.12	-15.42	↓	↓	↓
	LysoPC(18:3(6Z,9Z,12Z))	4.07	518.3233 (+)	$C_{26}H_{48}NO_7P$	1.02	12.70	↑	↑	↑
	Desaminotyrosine	3.47	167.1064 (+)	$C_9H_{10}O_3$	1.07	-14.22	↓	-	-
	Pipecolic acid	0.51	130.0868 (+)	$C_6H_{11}NO_2$	1.13	12.88	-	↑	↑
	Octadecanamide	14.57	284.2936 (+)	$C_{18}H_{37}NO$	1.09	14.62	-	↑	↑
	Cholesteryl acetate	17.03	429.3727 (+)	$C_{29}H_{48}O_2$	1.17	16.53	-	↑	↑
	Sphinganine	4.34	302.3056 (+)	$C_{18}H_{39}NO_2$	1.42	14.84	-	-	↑
	Eicosadienoic acid	15.15	309.2789 (+)	$C_{20}H_{36}O_2$	1.05	8.26	-	-	↑
	Eicosenoic acid	14.41	333.2794 (+)	$C_{20}H_{38}O_2$	1.10	13.92	-	-	↑
	Indolelactic acid	3.38	204.0665 (-)	$C_{11}H_{11}NO_3$	1.09	14.56	↑	↑	↑
	Gluconic acid	0.58	195.0506 (-)	$C_6H_{12}O_7$	1.07	-13.71	↓	↓	↓
	Pseudouridine	0.64	243.0619 (-)	$C_9H_{12}N_2O_6$	1.02	13.47	↑	↑	-
	12,13-DHOME	5.55	313.2383 (-)	$C_{18}H_{34}O_4$	1.05	12.09	↑	↑	↑
	5-HETE	8.19	319.2271 (-)	$C_{20}H_{32}O_3$	1.18	17.80	↑	↑	-
	Oleic acid	14.66	281.2487 (-)	$C_{18}H_{34}O_2$	1.15	12.82	-	-	↑
PG	Purine	6.42	121.0509 (+)	$C_5H_4N_4$	1.63	10.61	-	↑	-
	Indoxyl	0.55	156.0418 (+)	C_8H_7NO	1.08	-14.96	-	↓	↓
	9-cis-Retinoic acid	7.11	301.2159 (+)	$C_{20}H_{28}O_2$	1.20	-2.02	-	↓	-
	Sphinganine 1-phosphate	5.17	382.2724 (+)	$C_{18}H_{40}NO_5P$	1.03	13.89	-	↑	-
	PC(14:0/18:0)	14.62	734.5692 (+)	$C_{40}H_{80}NO_8P$	1.02	-15.44	-	↓	-
	PC(18:0/22:6)	14.24	856.5823 (+)	$C_{48}H_{84}NO_8P$	1.08	14.88	-	↑	-
	L-Alloisoleucine	0.926	130.0869 (-)	$C_6H_{13}NO_2$	1.17	-16.21	↓	↓	↓
	L-Tyrosine	0.799	180.0672 (-)	$C_9H_{11}NO_3$	1.15	-15.83	↓	↓	↓

Preprints (www.preprints.org) | NOT PEER-REVIEWED | Posted: 2 April 2018 doi:10.20944/preprints201804.0018.v1

12,13-DHOME	5.54	313.2386 (-)	$C_{18}H_{34}O_4$	1.22	12.35	↑	-	-
LPA(0:0/16:0)	6.46	409.2362 (-)	$C_{19}H_{39}O_7P$	1.09	14.57	↑	-	-
Tauroursodeoxycholic acid	4.20	498.2891 (-)	$C_{26}H_{45}NO_6S$	1.45	11.00	↑	-	-
Hippuric acid	3.06	178.0512 (-)	$C_9H_9NO_3$	1.08	13.78	↑	↑	-
Gluconic acid	0.59	195.0526 (-)	$C_6H_{12}O_7$	1.07	-13.71	↓	↓	-
Myristic acid	11.62	227.2024 (-)	$C_{14}H_{28}O_2$	1.09	-14.12	↓	↓	-
LysoPC(14:0)	5.702	466.2966 (-)	$C_{22}H_{46}NO_7P$	1.05	12.85	-	↑	-
UDP-glucuronate	5.25	579.0261 (-)	$C_{30}H_{48}O_{11}$	1.09	-14.05	-	↓	-
LPA(0:0/16:0)	6.51	409.2358 (-)	$C_{19}H_{39}O_7P$	1.09	14.06	-	↑	↑
Oleic acid	14.65	281.2487 (-)	$C_{18}H_{34}O_2$	1.37	12.82	-	-	↑

Preprints (www.preprints.org) | NOT PEER-REVIEWED | Posted: 2 April 2018 doi:10.20944/preprints201804.0018.v1

3.4 Metabolic pathway analysis

With these identified metabolites, an integrated metabolic pathway analysis was conducted by MetaboAnalyst 3.6. It revealed that three metabolic pathways including glycerophospholipid metabolism, pyrimidine metabolism and sphingolipid metabolism were associated with AM-induced mice, seven metabolic pathways including phenylalanine, tyrosine and tryptophan biosynthesis, pentose and glucuronate interconversions, tyrosine metabolism, starch and sucrose metabolism, sphingolipid metabolism, glycerolipid metabolism and glycerophospholipid metabolism were associated with PM-induced mice in Table 3 and Figure 4.

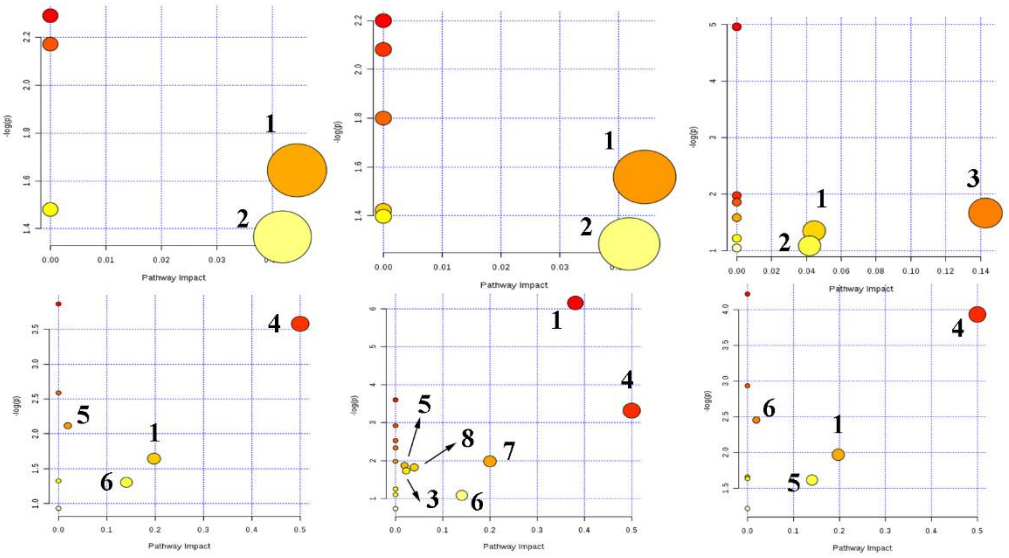

Figure 4. Summary of pathway analysis of biomarkers in plasma identified from AM and PG groups. Key:1, Glycerophospholipid metabolism; 2, Pyrimidine metabolism; 3, Sphingolipid metabolism; 4, Phenylalanine, tyrosine and tryptophan biosynthesis; 5, Glycerolipid metabolism; 6, Tyrosine metabolism; 7, Pentose and glucuronate interconversions; 8, Starch and sucrose metabolism.

Preprints (www.preprints.org) | NOT PEER-REVIEWED | Posted: 2 April 2018 doi:10.20944/preprints201804.0018.v1

Table 3 Metaboanalyst analysis of biomarkers in plasma identified from AM and PG groups.

Group	Pathway name	Total	Expected	Hits
LAM	**Glycerophospholipid metabolism**	**30**	**0.21171**	**1**
LAM	**Pyrimidine metabolism**	**41**	**0.28934**	**1**
LAM	beta-Alanine metabolism	17	0.11997	1
LAM	Arachidonic acid metabolism	36	0.25406	1
LAM	Pantothenate and CoA biosynthesis	15	0.10586	1
MAM	**Glycerophospholipid metabolism**	**30**	**0.23289**	**1**
MAM	**Pyrimidine metabolism**	**41**	**0.31828**	**1**
MAM	Lysine degradation	23	0.17855	1
MAM	Steroid biosynthesis	35	0.2717	1
MAM	Pantothenate and CoA biosynthesis	15	0.11644	1
MAM	Arachidonic acid metabolism	36	0.27946	1
MAM	beta-Alanine metabolism	17	0.13197	1
HAM	**Sphingolipid metabolism**	**21**	**0.20748**	**1**
HAM	**Glycerophospholipid metabolism**	**30**	**0.2964**	**1**
HAM	**Pyrimidine metabolism**	**41**	**0.40508**	**1**
HAM	Fatty acid biosynthesis	43	0.42484	1
HAM	Lysine degradation	23	0.22724	1
HAM	Steroid biosynthesis	35	0.3458	1
HAM	Pantothenate and CoA biosynthesis	15	0.1482	1
HAM	beta-Alanine metabolism	17	0.16796	1
HAM	Biosynthesis of unsaturated fatty acids	42	0.41496	3
LPG	**Phenylalanine, tyrosine and tryptophan biosynthesis**	**4**	**0.028229**	**1**
LPG	**Glycerophospholipid metabolism**	**30**	**0.21171**	**1**

 doi:10.20944/preprints201804.0018.v1

LPG	**Tyrosine metabolism**	**44**	**0.31052**	**1**	**0.27128**	**1.3046**	**0.14045**
LPG	**Glycerolipid metabolism**	**18**	**0.12703**	**1**	**0.12037**	**2.1172**	**0.0192**
LPG	Fatty acid biosynthesis	43	0.30346	1	0.26593	1.3245	0
LPG	Ubiquinone and other terpenoid-quinone biosynthesis	3	0.021171	1	0.021037	3.8615	0
LPG	Phenylalanine metabolism	11	0.077629	1	0.075203	2.5876	0
LPG	Aminoacyl-tRNA biosynthesis	69	0.48694	1	0.39397	0.93147	0
MPG	**Phenylalanine, tyrosine and tryptophan biosynthesis**	**4**	**0.036697**	**1**	**0.036233**	**3.3178**	**0.5**
MPG	**Glycerophospholipid metabolism**	**30**	**0.27523**	**3**	**0.0021248**	**6.1541**	**0.38086**
MPG	**Pentose and glucuronate interconversions**	**16**	**0.14679**	**1**	**0.13779**	**1.982**	**0.2**
MPG	**Tyrosine metabolism**	**44**	**0.40367**	**1**	**0.33757**	**1.086**	**0.14045**
MPG	**Starch and sucrose metabolism**	**19**	**0.17431**	**1**	**0.16159**	**1.8227**	**0.03958**
MPG	**Sphingolipid metabolism**	**21**	**0.19266**	**1**	**0.17711**	**1.731**	**0.02256**
MPG	**Glycerolipid metabolism**	**18**	**0.16514**	**1**	**0.15372**	**1.8726**	**0.0192**
MPG	Phenylalanine metabolism	11	0.10092	1	0.09674	2.3357	0
MPG	Arachidonic acid metabolism	36	0.33028	1	0.28537	1.254	0
MPG	alpha-Linolenic acid metabolism	9	0.082569	1	0.07982	2.528	0
MPG	Pentose and glucuronate interconversions	16	0.14679	1	0.13779	1.982	0
MPG	Fatty acid biosynthesis	43	0.3945	1	0.33125	1.1049	0
MPG	Ubiquinone and other terpenoid-quinone biosynthesis	3	0.027523	1	0.02729	3.6012	0
MPG	Linoleic acid metabolism	6	0.055046	1	0.053892	2.9208	0
MPG	Aminoacyl-tRNA biosynthesis	69	0.63303	1	0.47889	0.73628	0
HPG	**Phenylalanine, tyrosine and tryptophan biosynthesis**	**4**	**0.01976**	**1**	**0.019635**	**3.9305**	**0.5**
HPG	**Glycerophospholipid metabolism**	**30**	**0.1482**	**1**	**0.13939**	**1.9705**	**0.19753**
HPG	**Tyrosine metabolism**	**44**	**0.21736**	**1**	**0.19851**	**1.6169**	**0.14045**
HPG	**Glycerolipid metabolism**	**18**	**0.08892**	**1**	**0.085777**	**2.456**	**0.0192**
HPG	Biosynthesis of unsaturated fatty acids	42	0.20748	1	0.19028	1.6592	0

 doi:10.20944/preprints201804.0018.v1

HPG	Fatty acid biosynthesis	43	0.21242	1	0.19441	1.6378	0
HPG	Aminoacyl-tRNA biosynthesis	69	0.34086	1	0.29545	1.2192	0
HPG	Ubiquinone and other terpenoid-quinone biosynthesis	3	0.01482	1	0.014757	4.216	0
HPG	Phenylalanine metabolism	11	0.05434	1	0.053201	2.9337	0

Preprints (www.preprints.org) | NOT PEER-REVIEWED | Posted: 2 April 2018 doi:10.20944/preprints201804.0018.v1

Glycerophospholipid metabolism: Glycerophospholipids are important constituents of membranes of mammalian cells [30] which were reported to activate a variety of immune cells, including monocytes and neutrophils [31]. LysoPC(18:3(6Z,9Z,12Z)) is an intermediate in glycerophospholipid metabolism and it implied that increase of LysoPC(18:3(6Z,9Z,12Z)) may have a positive effect on long-term treated mice.

Pyrimidine metabolism: Pyrimidine compounds are widely distributed in mammalian animals and provide materials for a variety of mammalian metabolism throughout life. The promotion of cell proliferation is the main function of pyrimidine metabolism [32]. Uracil is a base of RNA [33] and also appears during DNA replication [34], playing an important role in protecting host from being attacked by pathogenic microorganisms [35].

Sphingolipid metabolism: Sphingolipid metabolism was found to affect immune function by binding CD1 proteins [36] and used as chemoattractant for immune cells [37]. CD4+ T cell function was typically regulated by sphingolipid metabolites in several ways such as regulation of T cell activation, survival and proliferation [38].

Phenylalanine, tyrosine and tryptophan biosynthesis & Tyrosine metabolism: When pathogenic microorganisms met their hosts, a series of self-protective strategy such as competition for nutrients was triggered. So, amino acid catabolism was used to prevent pathogen invasion and regulate immune responses [39]. Tyrosine is a precursor of protein tyrosine kinase [40] which could mediate immune system in a severe lymphoproliferative disorder mice model [41].

Glycerolipid metabolism: LPA (16:0/0:0) is a kind of fatty acid which is stored as energy in complex organisms and animals. Glycerolipid metabolism plays a role in maintaining body temperature by modulating glycerolipid fatty acid cycle in *vivo*. As a regulation mechanism during animal signing processes, it contains numerous formation and hydrolysis of glycerolipid and releases heat with the consumption of ATP [42].

Pentose and glucuronate interconversions & Starch and sucrose metabolism: Pentose and glucuronate provide numerous ribose 5-phosphate for nucleotide and nucleic acid synthetic reactions, playing an important role in cell metabolism [43]. UDP-glucose dehydrogenase is an essential process in pentose and glucuronate interconversions and UDP-glucose is converted to UDP-glucuronate [44]. When host was attacked, damaged cells will release UDP-glucose which trigger innate mucosal immune responses [45].

3.5 Immune-related correlation analysis

Previous studies mainly focused on detection and identification of biomarker [46, 47]. Diversity of identified endogenous substances were regarded as being most closely to experimental model, regulating related signaling pathways. The relation between biomarkers and metabolic pathways was more like the many-to-many logic relationship. But it is hard to explain which endogenous substance response for specific change in the internal environment. In this correlation analysis section, these mentioned difficulties were smoothly solved.

Preprints (www.preprints.org) | NOT PEER-REVIEWED | Posted: 2 April 2018 doi:10.20944/preprints201804.0018.v1

Correlations between detected metabolites and four pharmacodynamic indexes was analyzed by a bivariate correlation test. The relation between them was presented by pearson's correlation coefficient. A two-tailed test of significance using SPSS 24.0 software at significance levels of $p \leq 0.05$ and 0.01. The higher value of pearson's correlation coefficient, the closer relationship between them. In this way, immune-related metabonomic analysis was deduced (Figure 5 and Table 4). Glycerophospholipid metabolism was regulated in both AM and PG groups. Pyrimidine metabolism and sphingolipid metabolism were considered as the special pathway in AM groups. Energy metabolism and glycerolipid metabolism were the special pathway in PG groups.

In AM groups, the significant down regulation of uracil was found and it was negatively related closely to thymus index, indicating that uracil plays an important in cell proliferation in mice thymus. Uracil is a common naturally occurring pyrimidine found in RNA and also an essential key intermediate in adaptive immunity[48]. But, LysoPC(18:3(6Z,9Z,12Z)) and sphinganine may had an opposite effect on thymus, comparing to uracil. Meanwhile, LysoPC(18:3(6Z,9Z,12Z)) also had a positive effect on the proliferation of splenic lymphocytes and enhanced immunity by up regulation of LysoPC(18:3(6Z,9Z,12Z)). LysoPC(18:3(6Z,9Z,12Z)) is a lysophospholipid which have growth-related and -unrelated effects on lymphocytes and macrophages[49]. Besides, enhancement of spleen index was found in both LAM and MAM groups. In PG groups, much difference was found as compared to these in AM groups. Spleen index was enhanced by down regulation of UDP-glucuronate and up regulation of LPA(0:0/16:0). LysoPA(0:0/16:0) is a lysophosphatidic acid and mainly converted from lysophospholipids. Cytotoxic activity of NK cells and proliferation of splenic lymphocytes were found to have strong correlation with PC(14:0/18:0) in *vivo* and correlation coefficients were -0.98 and 0.88, respectively.

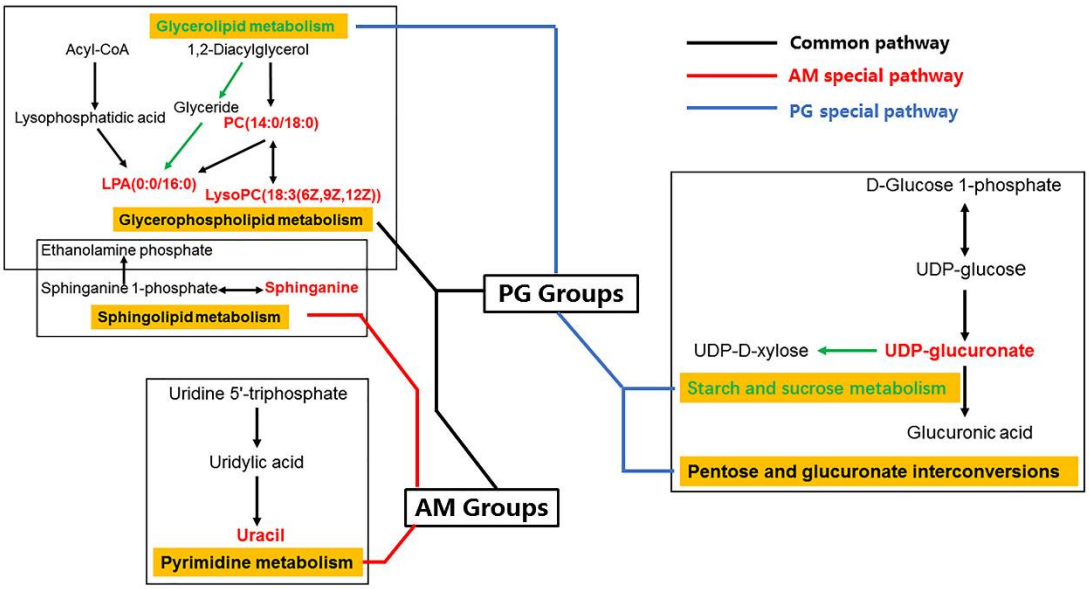

Figure 5. The similarities and differences of immune-related pathways analysis between AM and PG groups.

Preprints (www.preprints.org) | NOT PEER-REVIEWED | Posted: 2 April 2018 doi:10.20944/preprints201804.0018.v1

Table 4 List of correlation between biomarkers and pharmacodynamic indexes (** represents p <0.01, * represents p <0.05)

Group	Name	Rt (min)	m/z	Trend	Pearson Correlation Coefficient / Pharmacodynamic indexes			
					spleen Index	thymus index	cell proliferation rate	cytotoxic activity
LAM	Uracil	0.76	(+) 113.0342	↓	-	-0.63* / 0.91	-	-
LAM	LysoPC(18:3(6Z,9Z,12Z))	4.07	(+) 518.3233	↑	+0.66* / 3.57**	-	-	-
MAM	LysoPC(18:3(6Z,9Z,12Z))	4.06	(+) 518.3240	↑	+0.60* / 3.52*	-	-	-
HAM	LysoPC(18:3(6Z,9Z,12Z))	4.06	(+) 518.3238	↑	-	+0.54*/ 1.04	+0.55* / 0.25**	-
HAM	Sphinganine	4.34	(+) 302.3056	↑	-	+0.61*/ 1.04	-	-
LPG	LPA(0:0/16:0)	6.46	(-) 409.2362	↑	-	-	-	+0.66* / 71.7**
MPG	UDP-glucuronate	5.25	(-) 579.0261	↓	-0.64* / 3.95**	-	-	-
MPG	PC(14:0/18:0)	14.63	(+) 734.5692	↓	-	-	-0.98** / 0.26*	+0.88* / 28.5
HPG	LPA(0:0/16:0)	6.51	(-) 409.2356	↑	+0.71* / 3.98**	-	-	-

Preprints (www.preprints.org) | NOT PEER-REVIEWED | Posted: 2 April 2018 doi:10.20944/preprints201804.0018.v1

4. Conclusion

AM and PG were widely used for improving the immunity human beings in Chinese long history clinical practice, accompanying higher dosage and longer time usage. Metabonomics has brought out a comprehensive strategy in detecting and identifying biomarkers based on LC-MS/MS method, assessing experimental model in molecular level (microscopic scale). On the other hand, immunological indexes assessed experimental model in cellular and organ level (macroscopic scale).

In this study, immune-related metabonomics based on UPLC-Q/TOF-MS technique, pharmacodynamic evaluation and correlation analysis were used to investigate biomarkers and metabolic changes in mice with long-term administration of AM and PG. Pharmacodynamic results showed that both AM and PG could promote the spleen index , splenic lymphocyte and cytotoxic activity of natural killer (NK) cells. But, there was no significant change in thymus index.

To reveal the immunological profile and discriminate the differences between the AM and PG at the molecular level, a further plasma metabonomic study was conducted. Metabolomic data suggested that glycerophospholipid metabolism is the common metabolic pathway of AM and PG. Sphingolipid metabolism (biomarker: sphinganine) and pyrimidine metabolism (biomarker: uracil) associated significantly with immunity in AM-mice. Besides, glycerolipid metabolism (biomarker: LPA(0:0/16:0)) and energy metabolism (biomarker: UDP-glucuronate) (pentose and glucuronate interconversions, starch and sucrose metabolism) were much close to PG-mice. LysoPC (18:3(6Z,9Z,12Z))) is a biomarker in AM groups.

Finally, a novel comprehensive metabonomic analysis method is applied to clarify the scientific connotation of similar clinical effect of traditional Chinese medicine in improving immunity, opening a window for new drug development.

Acknowledgments: The authors are grateful for financial support from the Special Program for Major Subject of The China Academy of Chinese Medical Sciences during the Thirteen Five-year Plan Period (No. ZZ10-007) The funders had no role in study design, data collection and analysis, decision to publish, or preparation of the manuscript.

Author Contributions: Yuesheng Wang, Guoliang Xu and An Liu conceived and designed the experiments; Junqiu Liu performed the experiments and contributed to the acquisition of data and analyzed the data; Junqiu Liu wrote the paper; Sha Chen, Jun Zhang and Jintang Cheng contributed reagents/materials/analysis tools. All authors have revised the manuscript critically for important intellectual content and given final approval of the version to be published. Yuesheng Wang is responsible for the integrity of the work as a whole.

Conflicts of Interest: The authors declare no conflict of interest.

 doi:10.20944/preprints201804.0018.v1

Reference:

1. Lai, P. K.; Chan, J. Y.; Wu, S. B.; Cheng, L.; Ho, G. K.; Lau, C. P.; Kennelly, E. J.; Leung, P. C.; Fung, K. P.; Lau, C. B., Anti-inflammatory activities of an active fraction isolated from the root of Astragalus membranaceus in RAW 264.7 macrophages. *Phytother. Res.* **2014,** 28, (3), 395-404.

2. Elabd, H.; Wang, H. P.; Shaheen, A.; Yao, H.; Abbass, A., Astragalus membranaceus (AM) enhances growth performance and antioxidant stress profiles in bluegill sunfish (Lepomis macrochirus). *Fish Physiol. Biochem.* **2016,** 42, (3), 955-66.

3. Cho, W. C.; Leung, K. N., In vitro and in vivo anti-tumor effects of Astragalus membranaceus. *Cancer Lett.* **2007,** 252, (1), 43-54.

4. Yeh, T. S.; Chuang, H. L.; Huang, W. C.; Chen, Y. M.; Huang, C. C.; Hsu, M. C., Astragalus membranaceus improves exercise performance and ameliorates exercise-induced fatigue in trained mice. *Molecules* **2014,** 19, (3), 2793-807.

5. Li, M.; Wang, W.; Xue, J.; Gu, Y.; Lin, S., Meta-analysis of the clinical value of Astragalus membranaceus in diabetic nephropathy. *J. Ethnopharmacol.* **2011,** 133, (2), 412-9.

6. Mo, W. Y.; Lun, C. H. I.; Choi, W. M.; Man, Y. B.; Wong, M. H., Enhancing growth and non-specific immunity of grass carp and Nile tilapia by incorporating Chinese herbs (Astragalus membranaceus and Lycium barbarum) into food waste based pellets. *Environ. Pollut.* **2016,** 219, 475-482.

7. Chao, Y. H.; Wu, K. H.; Lin, C. W.; Yang, S. F.; Chao, W. R.; Peng, C. T.; Wu, H. P., PG2, a botanically derived drug extracted from Astragalus membranaceus, promotes proliferation and immunosuppression of umbilical cord-derived mesenchymal stem cells. *J. Ethnopharmacol.* **2017,** 207, 184-191.

8. Yang, F.; Xiao, C.; Qu, J.; Wang, G., Structural characterization of low molecular weight polysaccharide from Astragalus membranaceus and its immunologic enhancement in recombinant protein vaccine against systemic candidiasis. *Carbohydr. Polym.* **2016,** 145, 48-55.

9. Wang, Y.; Qian, X. J.; Hadley, H. R.; Lau, B. H., Phytochemicals potentiate interleukin-2 generated lymphokine-activated killer cell cytotoxicity against murine renal cell carcinoma. *Mol. Biother.* **1992,** 4, (3), 143-6.

10. McCulloch, M.; See, C.; Shu, X. J.; Broffman, M.; Kramer, A.; Fan, W. Y.; Gao, J.; Lieb, W.; Shieh, K.; Colford, J. M., Jr., Astragalus-based Chinese herbs and platinum-based chemotherapy for advanced non-small-cell lung cancer: meta-analysis of randomized trials. *J. Clin. Oncol.* **2006,** 24, (3), 419-30.

11. Shao, B. M.; Xu, W.; Dai, H.; Tu, P.; Li, Z.; Gao, X. M., A study on the immune receptors for polysaccharides from the roots of Astragalus membranaceus, a Chinese medicinal herb. *Biochem. Biophys. Res. Commun.* **2004,** 320, (4), 1103-11.

12. Lobina, C.; Carai, M. A.; Loi, B.; Gessa, G. L.; Riva, A.; Cabri, W.; Petrangolini, G.; Morazzoni, P.; Colombo, G., Protective effect of Panax ginseng in cisplatin-induced cachexia in rats. *Future Oncol.* **2014,** 10, (7), 1203-14.

13. Lei, Y.; Tao, L. L.; Wang, G. L., [Effect of extracts from Panax ginseng, Panax notoginseng, and Ligusticum chuanxiong on vascular smooth muscle cells of aging and hypertension rats]. *Zhongguo Zhong Xi Yi Jie He Za Zhi* **2012,** 32, (10), 1374-9.

14. Park, C. H.; Park, S. K.; Seung, T. W.; Jin, D. E.; Guo, T.; Heo, H. J., Effect of Ginseng (Panax ginseng) Berry EtOAc Fraction on Cognitive Impairment in C57BL/6 Mice under High-Fat Diet Inducement. *Evid. Based Complement. Alternat. Med.* **2015,** 2015, 316527.

15. Jiang, Y.; Li, Z.; Liu, Y.; Liu, X.; Chang, Q.; Liao, Y.; Pan, R., Neuroprotective effect of water extract of Panax ginseng on corticosterone-induced apoptosis in PC12 cells and its underlying molecule mechanisms. *J. Ethnopharmacol.* **2015,** 159, 102-12.

16. Borts, M. S.; Nikolaeva, E. G.; Kozhemiakina, N. V.; Borzova, I. V., [Anti-inflammatory and regenerative effect of geroprotector based on the extract from biomass of Panax ginseng]. *Adv Gerontol* **2011,** 24, (4), 701-6.

17. Liu, X. L.; Xi, Q. Y.; Yang, L.; Li, H. Y.; Jiang, Q. Y.; Shu, G.; Wang, S. B.; Gao, P.; Zhu, X. T.; Zhang, Y. L., The effect of dietary Panax ginseng polysaccharide extract on the immune responses in white shrimp, Litopenaeus vannamei. *Fish Shellfish Immunol.* **2011,** 30, (2), 495-500.

18. Shin, H. Y.; Jeong, H. J.; Hyo Jin, A.; Hong, S. H.; Um, J. Y.; Shin, T. Y.; Kwon, S. J.; Jee, S. Y.; Seo, B. I.; Shin, S. S.; Yang, D. C.; Kim, H. M., The effect of Panax ginseng on forced immobility time & immune function in mice. *Indian J. Med. Res.* **2006,** 124, (2), 199-206.

19. Lindon, J. C.; Holmes, E.; Nicholson, J. K., Metabonomics Techniques and Applications to Pharmaceutical Research & Development. *Pharm. Res.* **2006,** 23, (6), 1075-1088.

20. Qu, T.; Li, Z.; Zhao, S.; Li, A.; Qin, X., A metabonomic analysis reveals novel regulatory mechanism of Huangqi injection on leucopenia mice. *Immunopharmacol. Immunotoxicol.* **2016,** 38, (2), 113-23.

21. Li, C. Y.; Song, H. T.; Wang, X. X.; Wan, Y. Y.; Ding, X. S.; Liu, S. J.; Dai, G. L.; Liu, Y. H.; Ju, W. Z., Urinary metabolomics reveals the therapeutic effect of HuangQi Injections in cisplatin-induced nephrotoxic rats. *Sci. Rep.* **2017,** 7, (1), 3619.

22. Wu, W.; Jiao, C.; Li, H.; Ma, Y.; Jiao, L.; Liu, S., LC-MS based metabolic and metabonomic studies of Panax ginseng. *Phytochem. Anal* **2018**.

23. Lin, H.; Pi, Z.; Men, L.; Chen, W.; Liu, Z.; Liu, Z., Urinary metabonomic study of Panax ginseng in deficiency of vital energy rat using ultra performance liquid chromatography coupled with quadrupole time-of-flight mass spectrometry. *J. Ethnopharmacol.* **2016,** 184, 10-7.

24. Wu, L. R.; Shi, Z. F.; Gao, W. D.; Zhu, J. Y., Preliminary Metabonomic Analysis of Diabetic Rats Treated with Paired Extracts of Astragalus and Chinese Yams. *Advanced Materials Research* **2014,** 997, 288-291.

25. Zitti, B.; Molfetta, R.; Fionda, C.; Quatrini, L.; Stabile, H.; Lecce, M.; de Turris, V.; Ricciardi, M. R.; Petrucci, M. T.; Cippitelli, M.; Gismondi, A.; Santoni, A.; Paolini, R., Innate immune activating ligand SUMOylation affects tumor cell recognition by NK cells. *Sci. Rep.* **2017,** 7, (1), 10445.

26. Beltran, D.; Lopez-Verges, S., NK Cells during Dengue Disease and Their Recognition of Dengue Virus-Infected cells. *Front. Immunol.* **2014,** 5, 192.

27. Guan, H.; Moretto, M.; Bzik, D. J.; Gigley, J.; Khan, I. A., NK cells enhance dendritic cell response against parasite antigens via NKG2D pathway. *J. Immunol.* **2007,** 179, (1), 590-6.

28. Marcenaro, E.; Dondero, A.; Moretta, A., Multi-directional cross-regulation of NK cell function during innate immune responses. *Transpl. Immunol.* **2006,** 17, (1), 16-9.

29. Zhao, K. S.; Mancini, C.; Doria, G., Enhancement of the immune response in mice by Astragalus membranaceus extracts. *Immunopharmacology* **1990,** 20, (3), 225-33.

30. Hermansson, M.; Hokynar, K.; Somerharju, P., Mechanisms of glycerophospholipid homeostasis in mammalian cells. *Prog. Lipid Res.* **2011,** 50, (3), 240-57.

31. Nishioka, H.; Horiuchi, H.; Arai, H.; Kita, T., Lysophosphatidylcholine generates superoxide anions through activation of phosphatidylinositol 3-kinase in human neutrophils. *FEBS Lett.* **1998,** 441, (1), 63-6.

32. Marijnen, Y. M.; de Korte, D.; Roos, D.; van Gennip, A. H., Purine and pyrimidine metabolism of normal and leukemic lymphocytes. *Adv. Exp. Med. Biol.* **1989,** 253A, 433-8.

33. Lesk, A. M., Why does DNA contain thymine and RNA uracil? *J. Theor. Biol.* **1969,** 22, (3), 537-40.

34. Sire, J.; Querat, G.; Esnault, C.; Priet, S., Uracil within DNA: an actor of antiviral immunity. *Retrovirology* **2008,** 5, 45.

35. Maul, R. W.; Gearhart, P. J., Refining the Neuberger model: Uracil processing by activated B cells. *Eur. J. Immunol.* **2014,** 44, (7), 1913-6.

36. Huang, S.; Cheng, T. Y.; Young, D. C.; Layre, E.; Madigan, C. A.; Shires, J.; Cerundolo, V.; Altman, J. D.; Moody, D. B., Discovery of deoxyceramides and diacylglycerols as CD1b scaffold lipids among diverse groove-blocking lipids of the human CD1 system. *Proc. Natl. Acad. Sci. U. S. A.* **2011,** 108, (48), 19335-40.

37. Hannun, Y. A.; Obeid, L. M., Principles of bioactive lipid signalling: lessons from sphingolipids. *Nat. Rev. Mol. Cell Biol.* **2008,** 9, (2), 139-50.

38. Molano, A.; Huang, Z.; Marko, M. G.; Azzi, A.; Wu, D.; Wang, E.; Kelly, S. L.; Merrill, A. H., Jr.; Bunnell, S. C.; Meydani, S. N., Age-dependent changes in the sphingolipid composition of mouse CD4+ T cell membranes and immune synapses implicate glucosylceramides in age-related T cell dysfunction. *PLoS One* **2012,** 7, (10), e47650.

39. Grohmann, U.; Bronte, V., Control of immune response by amino acid metabolism. *Immunol. Rev.* **2010,** 236, 243-64.

40. Hubbard, S. R.; Till, J. H., Protein tyrosine kinase structure and function. *Annu. Rev. Biochem* **2000,** 69, 373-98.

41. Lu, Q.; Lemke, G., Homeostatic regulation of the immune system by receptor tyrosine kinases of the Tyro 3 family. *Science* **2001,** 293, (5528), 306-11.

42. Prentki, M.; Madiraju, S. R., Glycerolipid metabolism and signaling in health and disease. *Endocr. Rev.* **2008,** 29, (6), 647-76.

43. Sochor, M.; Baquer, N. Z.; McLean, P., Regulation of pathways of glucose metabolism in kidney. The effect of experimental diabetes on the activity of the

pentose phosphate pathway and the glucuronate-xylulose pathway. *Arch. Biochem. Biophys.* **1979,** 198, (2), 632-46.

44. Spicer, A. P.; Kaback, L. A.; Smith, T. J.; Seldin, M. F., Molecular cloning and characterization of the human and mouse UDP-glucose dehydrogenase genes. *J. Biol. Chem.* **1998,** 273, (39), 25117-24.

45. Arase, T.; Uchida, H.; Kajitani, T.; Ono, M.; Tamaki, K.; Oda, H.; Nishikawa, S.; Kagami, M.; Nagashima, T.; Masuda, H.; Asada, H.; Yoshimura, Y.; Maruyama, T., The UDP-glucose receptor P2RY14 triggers innate mucosal immunity in the female reproductive tract by inducing IL-8. *J. Immunol.* **2009,** 182, (11), 7074-84.

46. Zhang, Q.; Xu, G.; Li, J.; Guo, X.; Wang, H.; Li, B.; Tu, J.; Zhang, H., Metabonomic study on the plasma of streptozotocin-induced diabetic rats treated with Ge Gen Qin Lian Decoction by ultra high performance liquid chromatography-mass spectrometry. *J. Pharm. Biomed. Anal.* **2016,** 120, 175-80.

47. Yiqun, F.; Pu, Y.; Haitao, W.; Xiaochen, B.; Jun, M.; Shi, Z.; Yinghui, F., Metabonomic potential plasma biomarkers in abnormal fast buoyancy ascent escape-induced decompression sickness model and the protective effects of pyrrolidine dithiocarbamic acid. *Undersea Hyperb. Med.* **2017,** 44, (2), 109-119.

48. Doseth, B.; Visnes, T.; Wallenius, A.; Ericsson, I.; Sarno, A.; Pettersen, H. S.; Flatberg, A.; Catterall, T.; Slupphaug, G.; Krokan, H. E.; Kavli, B., Uracil-DNA glycosylase in base excision repair and adaptive immunity: species differences between man and mouse. *J. Biol. Chem.* **2011,** 286, (19), 16669-80.

 doi:10.20944/preprints201804.0018.v1

49. Gräler, M. H.; Goetzl, E. J., Lysophospholipids and their G protein-coupled receptors in inflammation and immunity. *Biochim. Biophys. Acta* **2002,** 1582, (1), 168-174.